UDC 62-83

https://doi.org/10.29202/nvngu/2019-6/13

V. A. Volkov, Cand. Sc. (Tech.), Assoc. Prof.,
orcid.org/0000-0003-1262-3988

Dnipro University of Technology, Dnipro, Ukraine, e-mail: green_stone@ukr.net

ENERGY-SAVING CONTROL FOR TRACTION FREQUENCY-REGULATED ASYNCHRONOUS ENGINE OF AN ELECTRIC VEHICLE

Purpose. Development of energy-saving control of a traction frequency-regulated asynchronous engine of an electric vehicle, investigation of its electro-mechanical and power processes.

Methodology. Methods of variational calculus, Runge-Kutta, mathematical analysis and interpolation, computer modeling.

Findings. Analytical dependencies are obtained to calculate the total power and energy losses for a traction frequency-regulated asynchronous engine (FRAE) under acceleration and deceleration regimes. With the help of these dependencies, quantitative assessment of the indicated power and energy losses was carried out, the electromechanical and energy processes of this FRAE for the proposed energy-saving and known (linear and parabolic) velocity trajectories were investigated.

Originality. Energy-efficient tachograms for traction FRAE with two control zones (with constant and weakened magnetic flux) are proposed, which allow minimizing its total energy loss in the start-braking regimes. Dependences are obtained which allow determining the energy-saving values of the speed of an electric vehicle in steady-state regimes.

Practical value. The application of the obtained results ensures a reduction in unproductive energy losses in the traction FRAE of the electric vehicle and an increase in the mileage of the latter on a single charge of the battery.

Keywords: *traction asynchronous engine, frequency regulation, energy-saving control, electric vehicle*

Introduction. Over the past decade, great attention has been paid all over the world to improving the technical characteristics and mastering the production of electric vehicles, which are usually created on the basis of frequency-regulated synchronous machines with permanent magnets or a short-circuited asynchronous engine. The reason for using a frequency-regulated asynchronous engine (FRAE) is the significant operational advantages associated primarily with the lack of need (as is required in a synchronous machine with permanent magnets) to conduct regular (periodic) tampering of the permanent magnets of this machine when operation of an electric vehicle. Taking into account the FRAE, the research on the energy regimes of this traction engine, the reduction of energy consumption in it is relevant and much needed.

Literature review. Publications, which have appeared in recent years in the foreign and domestic scientific and technical literature, offer a variety of approaches to energy-saving management of electric vehicles, created on the basis of frequency-regulated AC engines. In particular, in the article [1], by controlling the charge and discharge of the battery, a type of acceleration and deceleration tachograms was proposed, which reduced the electric energy consumption by an electric vehicle. In work [2], types of FRAE tachograms were proposed and investigated, at which the losses of this engine in acceleration and deceleration regimes with traction load in the range of super nominal speeds are minimized. In the publication [3], a strategy for managing a hybrid electric vehicle is developed and explored, in which a reduction in the total cost of gasoline and electricity consumed by this electric vehicle is achieved. In the article [4] for a racing hybrid car, tachograms were considered and investigated, ensuring its speed-limiting movement. In [5], scalar and vector control systems for traction FRAE are considered; experimental tachograms of an electric vehicle are shown during its acceleration and deceleration. In article [6], on the basis of completed research studies on regenerative braking regimes, recommendations for improving the energy efficiency of braking regimes of an electromobile are proposed. An analysis of the well-known publications suggests that they generally do not pay enough attention to studying electromechanical and energy processes as applied to the frequency-regulated asynchronous engine used as a traction engine for an electric vehicle, as well as to the energy-saving control of this engine.

Purpose. The purpose of the proposed article is to develop energy-saving control of a traction frequency-regulated asynchronous engine of an electromobile, the investigation of its electromechanical and energy-engineering processes.

Results. Basic assumptions:

- an idealized representation of a short-circuited three-phase FRAE was adopted, supplemented by taking into account the power loss in the steel of this engine [2];
- it is necessary to use the vector type of automatic control system (ACS) by an electric drive, which provides separate regulation of the magnetizing I_{1x} and active I_{1y} projections of the generalized stator current vector $\overline{I}_1$ (formed by the main harmonic components of the phase stator currents) of the engine on the axis a rotating orthogonal coordinate system "x–y", connected by the real axis "x" with the generalized flux linkage vector $\overline{\Psi}_r$ of the FRAE;
- we neglect the free (damped) components of the stator currents in the regimes of acceleration and deceleration (which is possible in practice with regard to the mentioned use of vector ACS due to their high speed and accuracy) [2];
- the object of the study was the energy and electromechanical processes for the traction FRAE with the proposed energy-saving control during acceleration and electric deceleration (with energy recovery in the battery) or uniform motion in the electric vehicle model (with characteristics from Table 1) [7];

- the absence of slipping between the driving wheels and the road surface was taken;

- FRAE parameters (active resistances of which were brought to a temperature of 115 °C) were unchanged (presented in Table 1);

- only the main components of the total power losses and the energy of the FRAE, caused by the main (first) harmonic components of the phase stator currents [2]), were considered;

- mathematical dependencies and subsequent calculations are performed in the relative system of units common to machines of alternating current (in which the nominal values of the stator frequency ω_{1n} and the synchronous speed of the rotor ω_n, as is well known, are identical to each other and are 1o. e., and the speeds for the considered FRAE ω_m, according to Table 1, are equal to 4000/1500 = 2.677 p. u.);

- in traction electric drive with acceleration and deceleration regimes by means of ACS, two control zones were implemented: in the first zone (with $0 \le \omega \le \omega_n$) – with a constant rotor flux coupling module Ψ_r equal to its nominal value Ψ_{rn}: $\Psi_r = \Psi_m = \text{const}$ and in the second (with $\omega_n \le \omega \le \omega_m$) – with a constant ratio: $\omega_1 \cdot \Psi_r = \omega_{1n} \cdot \Psi_{rn} = \text{const}$ [2].

At the first stage, we present the well-known analytical dependencies for determining the force F_r [N] of resistance to the movement of an electric vehicle, as well as the static moment of resistance M_r [p.u.] and moment of inertia J [kg·m^2] of an electric vehicle driven to the shaft of the traction engine [8]

$$\left.\begin{array}{ll} F_r = mg\left(\mu + i\right) + 0.5 C_a \rho_a S_f \upsilon^2; & \varepsilon = \omega\left[\text{rad/s}\right]/\upsilon \\ M_r = M_{ro} + q \cdot \omega^2; & J = J_r + m/\varepsilon^2 \\ M_{ro} = \dfrac{mg\left(\mu + i\right)}{\eta_m \cdot \varepsilon \cdot M_b}; & q = \dfrac{C_a \rho_a S_f \omega_b^2}{2 \cdot \eta_m \cdot \varepsilon^3 \cdot M_b} \end{array}\right\}, \quad (1)$$

Table 1

Nominal parameters of the engine and electric vehicle layout

The name of the parameter, measurements	Value
I Engine ATM 225 M4U2	
- power, kW	55
- effective linear voltage, V	450
- frequency of stator voltage, Hz	50
- rated / maximum speed, rpm	1500/4000
- slip, %	1.5
- torque, Nm	350
- multiplicity of starting moment	1.8
- the multiplicity of the maximum moment	3.5
- efficiency, %	92
- power factor	0.86
II Electric vehicle layout (based on Geely SC7 car)	
- the mass of the electric vehicle in the equipped state, kg	1400
- maximum speed, km/h	110
- acceleration time to speed of 100 km/h	15c
- coefficient of aerodynamic drag	0.35
- frontal projection area, m^2	2.1
- moment of inertia of rotating masses,kg·m^2	12
- rolling friction coefficient (asphalt)	0.01
- efficiency of the driving mechanism, %	97
- efficiency of the power converter, %	92
- battery capacity, kWh	22
- own power consumption not more than, kW	0.7

where υ is the speed of the electric vehicle, m/s; ω is the angular frequency of rotation (speed) of the rotor of the traction engine, p. u.; ε [rad/m] is the ratio between the respective speeds ω [rad/s] of the traction FRAE and the speed of the electric vehicle υ [m/s] (ε = const – for a particular type of electric vehicle); $\mu = 0.01$ is the coefficient of rolling friction; $C_a = 0.35$ is the coefficient of aerodynamic drag; $\rho_a = 1.226$ [kg/m^3] is the density of air (at a temperature of 15 ° C); $S_f = 2.1$ [m^2] is the frontal area of the electric vehicle; m [kg] is the mass of equipped electric vehicle; i [%] is longitudinal slope of the roadway; $g = 9.81$ [m/s^2] is acceleration of free fall; η_m is efficiency of the driving mechanism; values M_r, M_{ro}, q and ω are given in the system of relative units; ω_b [rad/s] and M_b [Nm] are basic values (for a relative system of units), respectively, of the rotor speed and the electromagnetic torque of the engine; $J_r = 12$ [kg · m^2] is the moment of inertia of all rotating parts of an electric vehicle (according to Table 1).

At the second stage, we will consider the analytical dependencies for calculating the total main power loss (TMPL) ΔP_{em} and the total main energy loss (TMEL) for the FRAE in acceleration and deceleration regimes, as well as the proposed energy-saving control of the electric vehicle in the specified regimes.

Taking into account the mentioned used two-zone speed control of the FRAE, the TMEL of this engine is calculated from the relationship

$$\Delta P_{en} = \begin{cases} \Delta P_{en.1} - \text{with} \;\; 0 \le \omega \le \omega_n & \left(\text{zone} \;\; 1\right) \\ \Delta P_{en.2} - \text{with} \;\; \omega_n < \omega \le \omega_m & \left(\text{zone} \;\; 2\right) \end{cases}, \quad (2)$$

where the values of current power losses $\Delta P_{en.1}$ and $\Delta P_{en.2}$, corresponding to zones 1 and 2 of regulation, are calculated from the ratios [2, 9]

$$\begin{aligned} \Delta P_{en.1} &= a_1 + b \cdot \left(M_r + J \cdot \omega'\right)^2 + c \left(\Psi_m / \Psi_{mn}\right)^2 \omega_1^{\lambda} + \\ &+ d \cdot \omega^2 \approx a_1 + b \cdot \left(M_r + J \cdot \omega'\right)^2 + c \cdot \omega^{\lambda} + d \cdot \omega^2; \end{aligned} \quad (3)$$

$$\begin{aligned} \Delta P_{en.2} &= a_2 \left(\frac{\Psi_m}{\omega_1} - \frac{T_r \Psi_m}{\omega_1^2} \omega_1'\right)^2 + b \omega_1^2 \left(M_r + J \cdot \omega'\right)^2 + \\ &+ c \left(\Psi_m / \Psi_{mn}\right)^2 \omega_1^{\lambda} + d \cdot \omega^2. \end{aligned} \quad (4)$$

In expressions (3) and (4), the following notation is used: ω and ω_1 – respectively, the rotor speed and angular frequency of the engine stator; ω' – derivative of rotor speed with respect to current time; $\lambda = 1.3$ – a coefficient that takes into account the change in power loss in steel FRAE from the stator frequency ω_1; Ψ_m and Ψ_{mn} – respectively, the current and nominal values of the modulus of the generalized magnetic flux vector in the air gap of the engine. The constant coefficients a_1, a_2, b, c, d are calculated from [2, 9].

TMEL during acceleration ΔW_a and deceleration ΔW_d for FRAE are determined from dependencies

$$\left.\begin{array}{ll} \Delta W_a = \Delta W_{a1} + \Delta W_{a2}; & \Delta W_d = \Delta W_{d1} + \Delta W_{d2} \\ \Delta W_{a1} = \int\limits_0^{t_{a1}} \Delta P_{en.1} \, dt; & \Delta W_{a2} = \int\limits_0^{t_{a2}} \Delta P_{en.2} \, dt \\ \Delta W_{d1} = \int\limits_0^{t_{d1}} \Delta P_{en.1} \, dt; & \Delta W_{d2} = \int\limits_0^{t_{d2}} \Delta P_{en.2} \, dt \end{array}\right\}, \quad (5)$$

where ΔW_{a1} and ΔW_{a2} are the values of TMEL for FRAE during acceleration, corresponding to the 1st and 2nd speed control zone; ΔW_{d1} and ΔW_{d2} are the values of the engine TMEL during deceleration, corresponding to the 1st and 2nd speed control zones; t_{a1} and t_{d1} are the duration of the acceleration and deceleration times for the first speed control zone (for $0 \le \omega \le \omega_n$);

t_{a2} and t_{d2} are the duration of the acceleration and deceleration times for the second control zone (at $\omega_n < \omega \le \omega_m$); t is the current time, which we determine to count from the beginning, for and within the limits of the zones of speed and acceleration ($0 \le t \le t_{a1}$ and $0 < t \le t_{a2}$) or deceleration ($0 \le t \le t_{d1}$ and $0 \le t < t_{d2}$) FRAE.

From the theory of variational calculus (for example, from the book by Andreeva V. A., Tsiruleva V. M. Variational calculus and optimization methods) it is known that while minimizing the integrals from (5) (or to minimize TMEL in the FRAE during acceleration and deceleration) the integrands of $\Delta P_{en.1}$ and $\Delta P_{en.2}$ from (3, 4) correspond to the Euler equation

$$\frac{\partial^2\left(\Delta P_{en}\right)}{\partial\omega'\cdot\partial\omega'}\omega'' + \frac{\partial^2\left(\Delta P_{en}\right)}{\partial\omega\cdot\partial\omega'}\omega' + \frac{\partial^2\left(\Delta P_{en}\right)}{\partial\omega\cdot\partial t} - \frac{\partial\left(\Delta P_{en}\right)}{\partial\omega} = 0, \quad (6)$$

where ω'' is the second derivative of the engine speed with respect to the current time t.

Substituting the values for the moment of resistance M_r from (1) into the final expression from (3), and then the resulting expression into equation (6), we transform the last into the form

$$\left.\begin{aligned} \omega'' &= K_1\cdot\omega + \left(\frac{2q^2}{J^2}\right)\omega^3 + \left(\frac{\lambda\cdot c}{2bJ^2}\right)\omega^{\lambda-1} \\ \text{where}\quad K_1 &= \left(2bqM_{ro} + d\right)\Big/ bJ^2 \end{aligned}\right\}, \quad (7)$$

corresponding to the regimes of acceleration and deceleration of the FRAE in the first speed control zone.

Due to the nonlinear form of the obtained differential equation from (7), it does not have an exact analytical solution. As shown by studies on numerical solutions of this equation, obtained by the Runge-Kutta method, they can be interpolated (with a relative standard deviation of less than 0.6 %) by velocity trajectories called "quasi optimal"

$$\left.\begin{aligned} \omega &= \omega_n\cdot\frac{\operatorname{sh}\left(\xi^*\sqrt{K_1}\cdot t\right)}{\operatorname{sh}\left(\xi^*\sqrt{K_1}\cdot t_{a1}\right)} \\ \omega &= \omega_n\frac{\operatorname{sh}\left[\xi^*\sqrt{K_1}\cdot\left(t_{d1}-t\right)\right]}{\operatorname{sh}\left(\xi^*\sqrt{K_1}\cdot t_{d1}\right)} \end{aligned}\right\}- \quad (8)$$

concave or

$$\left.\begin{aligned} \omega &= \omega_n\cdot\left\{1-\frac{\operatorname{sh}\left[\xi^*\sqrt{K_1}\cdot\left(t_{a1}-t\right)\right]}{\operatorname{sh}\left(\xi^*\sqrt{K_1}\cdot t_{a1}\right)}\right\} \\ \omega &= \omega_n\left\{1-\frac{\operatorname{sh}\left(\xi^*\sqrt{K_1}\cdot t\right)}{\operatorname{sh}\left(\xi^*\sqrt{K_1}\cdot t_{d1}\right)}\right\} \end{aligned}\right\}- \quad (9)$$

convex shape.

Similarly to the value considered for the moment of resistance M_r from (1) to expression (4), and then the resulting expression to Euler equation (6), considered in [2], quasi-optimal velocity trajectories for the second control zone were obtained FRAE

$$\left.\begin{aligned} \omega &= \omega_n + \left(\omega_m-\omega_n\right)\cdot\frac{\operatorname{sh}\left(\mathrm{x}^*\sqrt{\mathrm{K}_2}\times\mathrm{t}\right)}{\operatorname{sh}\left(\xi^*\sqrt{K_2}\cdot t_{a2}\right)} \\ \omega &= \omega_n + \left(\omega_m-\omega_n\right)\cdot\frac{\operatorname{sh}\left[\xi^*\sqrt{K_2}\cdot\left(t_{d2}-t\right)\right]}{\operatorname{sh}\left(\xi^*\sqrt{K_2}\cdot t_{d2}\right)} \end{aligned}\right\}- \quad (10)$$

concave or

$$\left.\begin{aligned} \omega &= \omega_n + \left(\omega_m-\omega_n\right)\cdot\left\{1-\frac{\operatorname{sh}\left[\xi^*\sqrt{K_2}\cdot\left(t_{a2}-t\right)\right]}{\operatorname{sh}\left(\xi^*\sqrt{K_2}\cdot t_{a2}\right)}\right\} \\ \omega &= \omega_n + \left(\omega_m-\omega_n\right)\cdot\left\{1-\frac{\operatorname{sh}\left(\xi^*\sqrt{K_2}\cdot t\right)}{\operatorname{sh}\left(\xi^*\sqrt{K_2}\cdot t_{d2}\right)}\right\} \end{aligned}\right\}- \quad (11)$$

convex shape, where $K_2 = d\cdot\Psi_{rn}^2/bJ^2$.

Moreover, the first dependencies from the systems (8, 9) and (10, 11) correspond to acceleration, and the second – to deceleration of the FRAE. In these dependencies, the value of the corrective coefficient ξ^* corresponds to the minimum possible value of the TMEL for the FRAE found from dependencies (3, 4), respectively, for the first and second speed control zones.

After substituting expressions (8–11), dependences (3, 4) were calculated from (5) TMEL values: ΔW_{a1}, ΔW_{a1} – by varying the acceleration t_{a1} and deceleration t_{d1} times in the first speed zone of the electric vehicle (for $\upsilon_n = 41.25$ km/h speed); ΔW_{a2}, ΔW_{d2} – by varying the acceleration t_{a2} and deceleration t_{d2} times in the second zone of the electric vehicle speeds (for $\upsilon_m = 50$ km/h and $\upsilon_m = 100$ km/h speeds), which are depicted as graphs in Figs. 1 and 2. In these and subsequent figures, we agree to designate numbers: *1* and *2* – values referring to quasi-optimal trajectories of speed, respectively, of a concave and convex shape; *3* and *4* – to parabolic trajectories of speed, respectively, of a concave and convex shape; *5* – to the linear trajectory of speed. Graphic dependencies for the coefficient ξ^* are shown in Fig. 3.

According to the results of the performed calculations, the values of the optimal acceleration time t_{a1}^o, t_{a2}^o and deceleration t_{d1}^o, t_{d2}^o and the corresponding optimal (minimum) values of the TMEL ΔW_{a1}^o, ΔW_{a2}^o and ΔW_{d1}^o, ΔW_{d2}^o for FRAE with considered different trajectories of speed (moreover, in Table 3 – for $\upsilon_m = 50$ km/h and $\upsilon_m = 100$ km/h speeds), as well as values of specific energy losses Δp_{a1}, Δp_{a2} and Δp_{d1}, Δp_{d2} for FRAE when moving α_{a1}, α_{a2} and α_{d1}, α_{d2} its rotor in acceleration and deceleration regimes in the regulation zones *1* and *2*

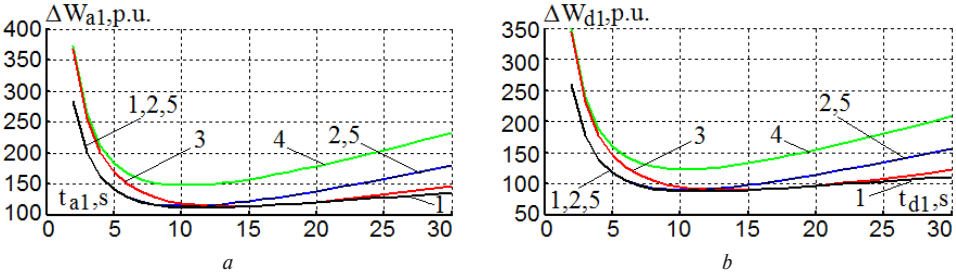

Fig. 1. Dependences of the MEEL ΔW_{a1}, ΔW_{d1} for traction FRAE (with m = 1400 kg, i = 0.02, υ_n = 41.25 km/h) in the first control zone with varying acceleration (a) and deceleration time (b) for:

1 and 2 – quasi-optimal concave and convex; 3 and 4 – parabolic concave and convex; 5 – linear tachograms

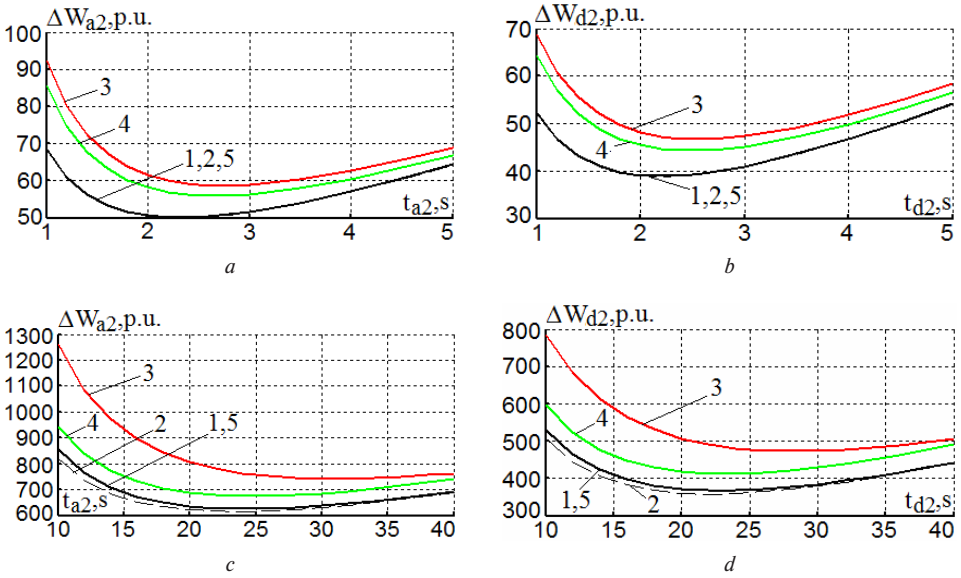

Fig. 2. Dependences of the MEEL ΔW_{a1}, ΔW_{d1} for traction FRAE (for m = 1400 kg, i = 0.02) in the second control zone (at maximum speeds υ_m equal to:

a, b – 50 km/h; c, d – 100 km/h with varying acceleration time (a , c) and deceleration time (b, d) for: 1 and 2 – quasi-optimal concave and convex; 3 and 4 – parabolic concave and convex; 5 – linear tachograms

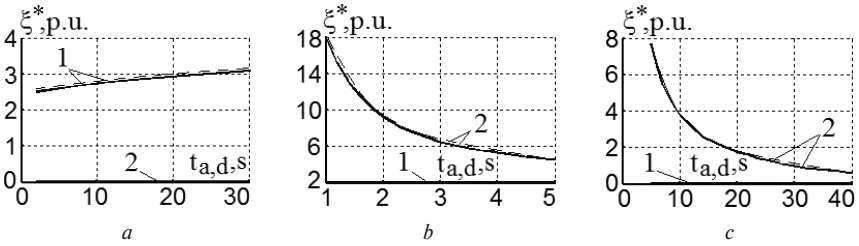

Fig. 3. Dependencies $\xi^*(t_{a1})$, $\xi^*(t_{d1})$ and $\xi^*(t_{a2})$, $\xi^*(t_{d2})$ for quasi-optimal concave tachograms 1 and convex 2 form at the first (a) and second (b, c) control zones and speed values:

a – υ_n = 41.25 km/h; b – υ_m = 50 km/h; c – υ_m = 100 km/h

$$\left.\begin{array}{lll} \Delta p_{a1} = \Delta W^o_{a1}/\alpha_{a1}; & \Delta p_{d1} = \Delta W^o_{d1}/\alpha_{d1} & \\ \Delta p_{a2} = \Delta W^o_{a2}/\alpha_{a2}; & \Delta p_{d2} = \Delta W^o_{d2}/\alpha_{d2} & \\ \alpha_{a1} = \int\limits_0^{t^o_{a1}} \omega \cdot dt; & \alpha_{d1} = \int\limits_0^{t^o_{d1}} \omega \cdot dt; & \alpha_{a2} = \int\limits_0^{t^o_{a2}} \omega \cdot dt \\ \alpha_{d2} = \int\limits_0^{t^o_{d2}} \omega \cdot dt; & t^o_a = t^o_{a1} + t^o_{a2}; & t^o_d = t^o_{d1} + t^o_{d2} \end{array}\right\}, \quad (12)$$

where t^o_a and t^o_d are the resulting optimal acceleration and deceleration time of the electric vehicle.

Table 4 shows the calculated values

$$\Delta W_a = \Delta W_{a1} + \Delta W_{a2}; \quad \Delta p_a = \Delta W_a/(\alpha_{a1} + \alpha_{a2});$$

$$\Delta W_d = \Delta W_{d1} + \Delta W_{d2}; \quad \Delta p_d = \Delta W_d/(\alpha_{d1} + \alpha_{d2}).$$

TMEL ΔW_a, ΔW_d and specific losses Δp_a, Δp_d, the energy of the FRAE during acceleration and deceleration of an electric engine (for υ_m = 50 km/h, i = 0.02) at optimal and non-optimal acceleration and deceleration time: $t_a = t_d$ = 5 s (where $t_{a1} = t_{d1}$ = 4 s, $t_{a2} = t_{d2}$ = 1 s).

For optimal acceleration and deceleration time from Tables 2 and 3 (at υ_m = 100 km/h), they are calculated from dependencies (1–5), (8–11) electromechanical (speed ω and position α of the engine shaft, speed υ of the electric vehicle) and energy (general main power ΔP_{en} and energy losses ΔW_a, ΔW_d), transients of the engine, which are shown in Fig. 4. Also shown in this figure are transients for the electromagnetic moment M and absolute slip β, the position s of the electric vehicle, the modules of the generalized rotor flux linkage vectors Ψ_r, the magnetic flux Ψ_m in the air gap and the stator current I_1 FRAE, calculated from the known dependencies [2]

Table 2

Optimum time t^o_{a1}, t^o_{d1} and TMEL ΔW^o_{a1}, ΔW^o_{d1}, specific losses Δp_{a1}, Δp_{d1} of energy during acceleration and deceleration of the FRAE in the first zone of regulation (for m = 1400 kg, i = 0.02, υ_n = 41.25 km/h)

Number of tachogram	Regulation zone 1 (with υ_n = 41.25 km/h)					
	t^o_{a1}	ΔW^o_{a1}	Δp_{a1}	t^o_{d1}	ΔW^o_{d1}	Δp_{d1}
Units	s	p.u.	p.u.	s	p.u.	p.u.
1	11.4	110.94	0.0734	11.4	86.89	0.0575
2	10.2	114.34	0.0714	10.2	90.30	0.0564
3	13.7	113.59	0.0792	13.7	89.54	0.0624
4	10.2	147.41	0.0690	10.3	123.4	0.0572
5	10.2	114.35	0.0714	10.2	90.30	0.0564

Table 3

Optimal time t^o_{a1}, t^o_{d1} and TMEL ΔW^o_{a1}, ΔW^o_{d1}, specific losses Δp_{a1}, Δp_{d1} of energy during acceleration and deceleration of the FRAE in the second zone regulation (for m = 1400 kg, i = 0.02, υ_m = 50 km/h and υ_m = 100 km/h)

Number of tachogram	Zone regulation *2* (with υ_m = 50 km/h)						Zone regulation *2* (with υ_m = 100 km/h)					
	t^o_{a2}	ΔW^o_{a2}	Δp_{a2}	t^o_{d2}	ΔW^o_{d2}	Δp_{d2}	t^o_{a2}	ΔW^o_{a2}	Δp_{a2}	t^o_{d2}	ΔW^o_{d2}	Δp_{d2}
Measurements	s	p.u.	p.u.	s	p.u.	p.u.	s	p.u.	p.u.	s	p.u.	p.u.
1	2.27	50.10	0.0636	2.19	38.91	0.0512	24.2	625.41	0.0481	22.8	367.05	0.0299
2	2.27	50.00	0.0632	2.19	38.82	0.0509	23.3	615.52	0.0469	22.2	358.36	0.0287
3	2.77	58.58	0.0565	2.53	46.69	0.0549	31.0	741.91	0.0517	28.5	472.79	0.0358
4	2.64	56.01	0.0592	2.52	44.34	0.0491	24.8	674.34	0.0444	23.2	412.86	0.0291
5	2.27	50.10	0.0636	2.19	38.91	0.0512	24.2	625.41	0.0481	22.8	367.05	0.0299

Table 4

TMEL ΔW_a, ΔW_d and specific losses Δp_a, Δp_d the energy of the FRAE during acceleration and deceleration (for m = 1400 kg, i = 0.02, υ_m = 50 km/h) with optimal and non-optimal durations of acceleration and deceleration times

Number of tachogram	For optimal times						For times: $t_a = t_d$ = 5 s			
	t^o_a	ΔW^o_a	Δp_a	t^o_d	ΔW^o_d	Δp_d	ΔW_a	Δp_a	ΔW_d	Δp_d
Measurements	s	p.u.	p.u.	s	p.u.	p.u.	p.u.	p.u.	p.u.	p.u.
1	13.67	161.04	0.1370	13.59	125.80	0.1087	230.83	0.2615	190.62	0.2537
2	12.47	164.34	0.1346	12.39	129.12	0.1073	230.77	0.2510	190.63	0.2466
3	16.47	172.17	0.1357	16.23	136.23	0.6789	293.23	0.3536	245.46	0.3509
4	12.84	203.42	0.1282	12.82	167.74	0.1063	297.75	0.2920	252.38	0.2906
5	12.47	164.45	0.1350	12.39	129.21	0.1076	231.01	0.2523	190.80	0.2479

$$\left.\begin{array}{ll} M = M_r + J\omega'; & \beta = R_r \cdot M / \Psi_r^2 \\ \Psi_r = \begin{cases} \Psi_m - \text{for zone 1} \\ \Psi_m / \omega - \text{for zone 2} \end{cases}; & s = \int_0^t \alpha \cdot dt \\ I_{1x} = \left(\Psi_r + T_r \cdot \Psi'_r\right) / L_m; & I_{1y} = M / k_r L_m \\ \Psi_{mx} = k_r \left(\Psi_r + L_{\sigma r} \cdot I_{1x}\right); & \Psi_{my} = k_r L_{\sigma r} \cdot I_{1y} \\ I_1 = \left(I_{1x}^2 + I_{1y}^2\right)^{0.5}; & \Psi_m = \left(\Psi_{mx}^2 + \Psi_{my}^2\right)^{0.5} \end{array}\right\}, \quad (13)$$

where I_{1x}, I_{1y} and Ψ_{mx}, Ψ_{my} are the projections of the generalized vectors of the stator current $\overline{I}_1$ and the flow $\overline{\Psi}_m$ in the air gap of the engine on the axis of the rotating orthogonal coordinate system "x–y"; T_r, $L_{\sigma r}$ and k_r are electromagnetic time constant, inductance of scattering and coupling coefficient of the engine rotor; L_m is magnetization inductance.

At the third stage, we will consider the energy-saving control of an electric vehicle when it is moving at a uniform speed (υ = const) and with a constant inclination (i = const) of the roadway. Taking into account the relations from (1), this obviously corresponds to constant values of the angular velocity ω = const and the static torque M_r = const of the engine.

For the steady-state FRAE regimes, we will give (according to the book Pivnyak G. G., Volkov A. V. Modern frequency-regulated asynchronous electric drives with pulse-width modulation) the optimal (minimum possible) ratio χ_o between the main electromagnetic power losses ΔP_{em} and the module $|M|$ of the developed electromagnetic moment M of this engine

$$\left.\begin{array}{l} \chi_o = 2 \cdot \left(X \cdot Y\right)^{0.5} / k_r L_m = \Delta P_{em} / M = \min \\ X = R_s + 0.005 \dfrac{P_n}{\eta_n} + k_r^2 \left(R_r + \dfrac{\Delta P_{st.n} L_{\sigma r}^2 \omega_1^{\lambda}}{\Psi_{mn}^2} \right) \\ Y = R_s + 0.005 P_n / \eta_n + \Delta P_{st.n} L_m^2 \omega_1^{1.3} / \Psi_{mn}^2 \end{array}\right\}, \quad (14)$$

where R_s and $\Delta P_{st.n}$ are stator resistance and nominal power loss in steel FRAE; P_n and η_n are rated power and engine efficiency.

This regime corresponds to the optimal value of the absolute slip β_o and the angular frequency of the stator ω_1 FRAE, calculated from the expressions

$$\beta_o = \pm \frac{1}{T_r} \left[\frac{Y}{X} \right]^{0.5}; \quad \omega_1 = \omega + \beta_o; \quad T_r = \frac{\left(L_m + L_{\sigma r}\right)}{R_r}, \quad (15)$$

where of double characters: the upper character refers to the engine, and the lower – to the generator regime of the engine.

Based on the second relation in (13) for absolute slip β of the FRAE, we obtain, taking into account (15) for the considered optimal steady state, the dependence connecting the electromagnetic torque M and the optimal value Ψ_{ro} of the motor rotor flux linkage

$$\Psi_{ro} = \sqrt{R_r |M| / |\beta_o|} = \sqrt{\left(L_m + L_{\sigma r}\right) \cdot |M|} \cdot \left[X / Y \right]^{1/4}. \quad (16)$$

In the specified optimal regime, which minimizes the basic electromagnetic ΔP_{em} and total power losses ΔP_{en} of the engine, these power losses are calculated taking into account (14) in the form

$$\left.\begin{array}{l} \Delta P_{em} = \chi_o |M| = 2 |M| \left(X / Y\right)^{0.5} / k_r L_m \\ \Delta P_{en} = \Delta P_{em} + d \cdot \omega^2 \end{array}\right\}. \quad (17)$$

In the context of an electric vehicle, it is of interest to minimize the specific total energy p_Σ consumed when moving the shaft of the FRAE in installed (with uniform speed ω = const and length of time t_{st}) driving regimes

$$\left.\begin{array}{l} p_\Sigma = \dfrac{P_\Sigma \cdot t_{st}}{\alpha} = \dfrac{P_\Sigma \cdot t_{st}}{\omega \cdot t_{st}} = \dfrac{P_\Sigma}{\omega} = \min \\ P_\Sigma = \left(M_r \cdot \omega + \Delta P_{en}\right) / \eta_{pc} + P_{on} \end{array}\right\}, \quad (18)$$

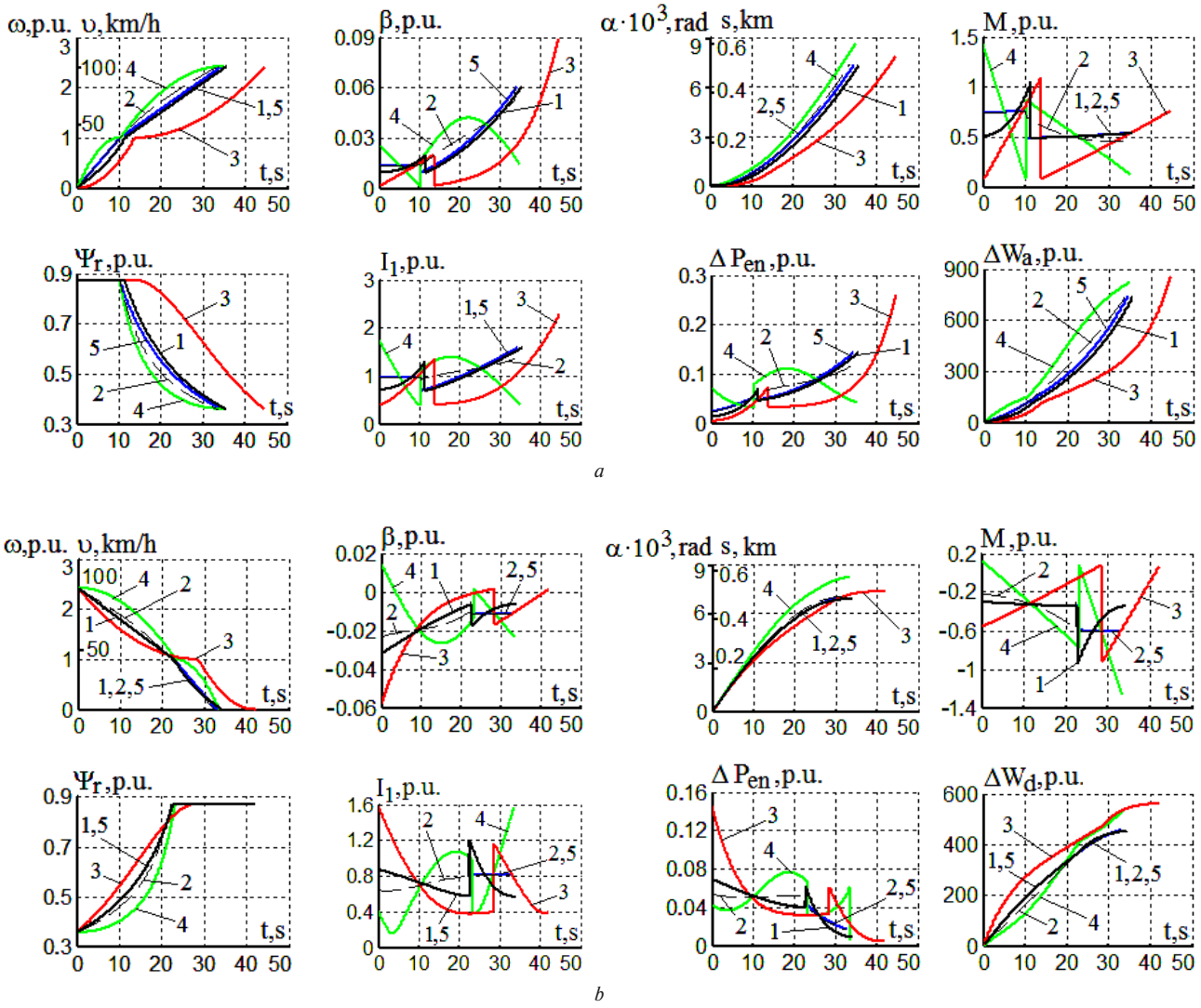

Fig. 4. Electromechanical and energy transient processes of traction FRAE (with m = 1400 kg, i = 0.02, υ_m = 100 km/h) with optimal acceleration time (a) and braking time (b) for 1 and 2 – quasi-optimal concave and convex, 3 and 4 – parabolic concave and convex, 5 – linear tachograms

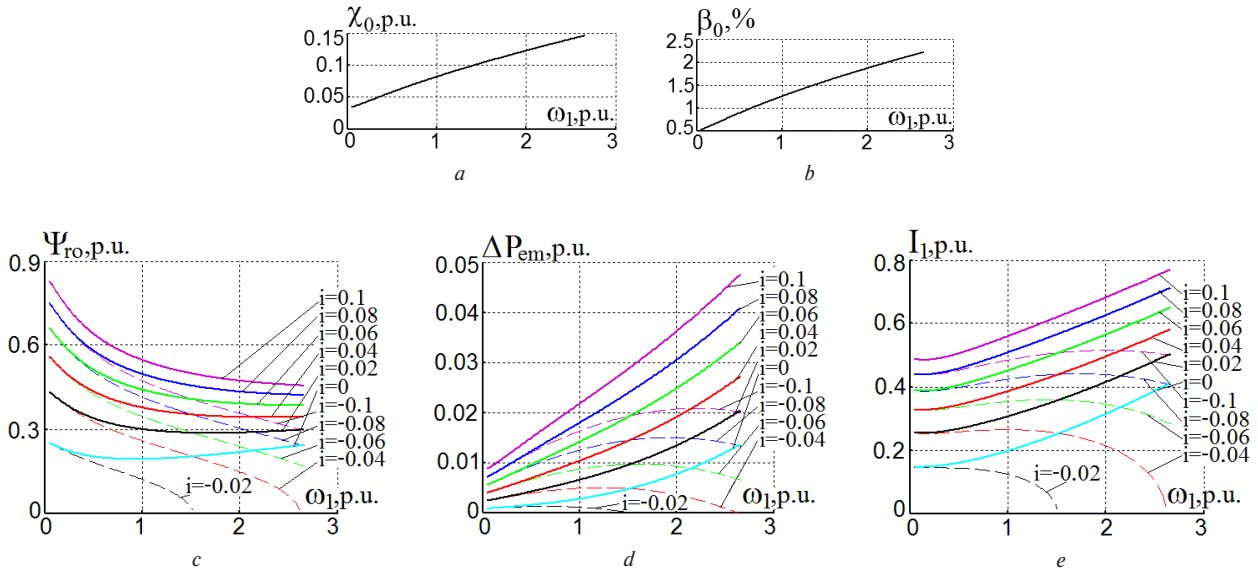

Fig. 5. Change in the values of χ_o, Ψ_{ro}, β_o, I_1 and ΔP_{em} traction FRAE in the optimal steady state

where α is the specified movement of the engine shaft during this steady motion; P_{on} is the active power consumption of the own needs (ON) of an electric vehicle (spent on powering the onboard computer, alarm systems, lighting, etc.).

Note that in the absence of slippage of the driving wheels of the electric vehicle relative to the road surface, the movement of the shaft of the FRAE is directly proportional to the movement of the electric vehicle: $\alpha = \varepsilon \cdot s$. From formulas (13–17), the following dependences are calculated and plotted as graphs in Fig. 5: parameter χ_o, optimal absolute slip β_o, module of generalized rotor flux linkage Ψ_{ro} and stator current I_1, basic electro-magnetic power losses $\Delta P_{??}$ of the FRAE as a function of frequency ω_1 of the stator. From (18), the values of the specific total energy p_Σ consumed by the electric vehicle are shown for different values of its speed υ, engine speed ω and road slope i in Fig. 6, calculated for the steady state operation of the electric vehicle. Figs. 5 and 6 show the following: a solid line of graphics is related to the engine, and a dotted line – to the generator regime of operation of the FRAE. The minimum values of the specific energy p_Σ consumed in total energy in Fig. 6 correspond to energy-saving speeds υ^* and ω^* of an electric vehicle or engine.

In order to proceed with the evaluation of electromechanical and energy processes from relative to absolute values, the values obtained in relative units should be multiplied by the basic values given for the FRAE in Table 5.

A quantitative estimate of the possible range of an electric vehicle (for a specific value of the established speed υ and on one charge of the battery) is determined from the expression [8]

$$s = \sum s_{a,d} + s_{st} = \sum s_{a,d} + \\ + \upsilon \frac{\left(W_{AB} + W_G\right) \cdot \eta_{pc} - \sum W_{a,d} - \left(P_{on} \cdot \eta_{pc} + \Delta P_{\text{mod}}\right) \cdot \sum t_{a,d}}{P_{on} \cdot \eta_{pc} + M_r \cdot \omega + \Delta P_{en} + \Delta P_{\text{mod}}}, \quad (19)$$

where $\sum s_{p,m}$ is the total distance traveled by the electric vehicle in the start-stop regimes, m; s_{st} is the distance traveled by the electric vehicle in the steady state (at a constant speed: υ = const) regime; W_{AB} is initial charge of the accumulator battery, kJ; W_G is battery charge replenishment with generated energy, kJ (in the absence of generation: $W_G = 0$); $\Delta P_{\text{mod}} \approx = \tau_m \cdot \Delta P_{en.n}$ is modulation power losses of FRAE, caused by high-frequency harmonics of its phase stator currents (where $\tau_m \approx 0.03$); ΔP_{en} is nominal power loss FRAE; η_{pc} is efficiency of the power converter that feeds the traction FRAE.

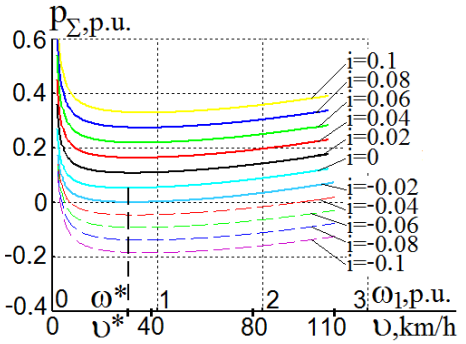

Fig. 6. Specific total consumption (shown by a solid line) and generation (shown by a dotted line) of the energy of the FRAE of an electric vehicle

For the considered model of an electric vehicle (with a mass of 1.400 kg), moving along a horizontal stretch of road in the modes of initial acceleration and the next steady motion with a constant speed of 100, 60 or 16.6 km/h, mileage on a full battery charge, – read from (19) is 119, 214 and 208 km, respectively, and at the optimum value (from Fig. 6) of the $\upsilon^* = 29.7$ km/h speed, the maximum possible value is 242 km.

Conclusions.

1. The developed energy-saving control in acceleration and deceleration regimes, which consists in the quasi-optimal tachogram form (8–11) for the first and second speed control zones of the FRAE, allows, according to Figs. 1 and 2 compared with other types tachograms, reducing the TMEL engine (depending on the length of time of acceleration and deceleration) from 5 to 50 %.

2. According to Figs. 1 and 2, "U"-form of the dependencies of the TMEL ΔW_{a1}, ΔW_{a2} and ΔW_{d1}, ΔW_{d2} for the FRAE on the duration of its acceleration t_{a1}, t_{a2} and deceleration t_{d1}, t_{d2} time is installed, for the first and second speed control zones. As follows from Table 4, during the transition to the optimum acceleration t_a^o and t_d^o deceleration time, a reduction in the total effective electrical power output of the traction FRAE by 30–35 % is provided.

3. It was revealed that with optimal durations of acceleration t_{a1}^o, t_{a2}^o, t_a^o and deceleration t_{d1}^o, t_{d2}^o, t_d^o time, the smallest, according to Tables 2–4, ratios Δp_{a1}, Δp_{d1} and Δp_{a2}, Δp_{d2} from (12) or Δp_a^o between Δp_d^o TMEL and movements of the shaft FRAE are inherent in the parabolic form of the convex shape of the tachogram (TG). It should be noted that this type of TG, due to possible unacceptably high values of the derivative velocity and jerk at the beginning of acceleration and deceleration, may not be applicable for passenger traffic [10] (their area of use is usually limited to racing cars [4]), and therefore quasi-optimal TGs are more preferable (with lower values of the derivative velocity and jerk and good energy-saving properties).

4. The proposed energy-saving control in steady-state electric vehicle regimes, which consists in optimal control of the minimum basic electromagnetic power losses of the FRAE and setting the optimum speed ω^* of the engine or electric vehicle υ^* (corresponding to (18) and Fig. 6 minimum ratio p_Σ) provides the greatest mileage of the electric vehicle or generation energy when moving at a uniform speed.

5. According to dependence (19), the transition from υ = = 100 km/h speed to its optimal (energy saving) $\upsilon^* = 29.7$ km/h value (using the example of the electric vehicle under consideration, for example $i = 0$) increases this mileage by 2 times at the initial charge of the battery.

6. The proposed energy-saving traction control FRAE is recommended as an economical control in existing electric vehicles, especially those operated in rural areas with low-intensity traffic (when high performance is not required from an electric vehicle in acceleration and deceleration regimes), as well as for electric vehicles.

Table 5

Basic values of engine magnitudes

Magnitude	I_1	M, M_r	Ψ	ω_1	ω	P, ΔP	ΔW	R_s, R_r	L	J	t
Dimension	A	Nm	Wb	rad/s	rad/s	kW	J	Om	mH	kg·m^2	s
Value	126	443	1.17	100π	50π	69.52	221.3	2.913	9.27	0.00897	0.01/π

References.
1. Dongbin, L., & Minggao, O. (2014). Torque-based Optimal Acceleration Control for Electric Vehicle. Chinese journal of mechanical engineering, *27*, 319-330.
2. Volkov, V.A. (2019). Energy-saving tachograms acceleration (deceleration) of a frequency-regulated asynchronous engine for super nominal speeds. *Naukovyi Visnyk Natsionalnoho Hirnychoho Universytetu*, (4), 55-62. https://doi.org/10.29202/nvngu/2019-4/11.
3. Patil, R.M., Filipi, Z., & Fathy, H.K. (2013). Comparison of Supervisory Control Strategies for Series Plug-In Hybrid Electric Vehicle Power trains Through Dynamic Programming. IEEE Transactions on control systems technology, 1-8.
4. Ebbesen, S., Salazar, M., Elbert, Ph., Bussi, C., & Onder, Ch. H. (2017). Time-optimal Control Strategies for a Hybrid Electric Race *Car. IEEE Transactions on control systems technology*, 1-15.
5. Livinţ, G., Horga, V., Răţoi, M., & Albu, M. (2011). Control of Hybrid Electrical Vehicles. *Electric Vehicles – Modelling and Simulations*, 41-66.
6. Klepikov, V.B., & Semikov, A.V. (2017). Energy efficiency regenerative modes of the electric vehicle. *Tehnichna electrodinamica*, (6), 36-42.
7. Poddubko, V.B., Belevich, A.V., & Adashkevich, V.I. (2017). Electric vehicle mockup: stages of creation and first results. *Mekhanika mashin, mekhanizmov i materialov, 4*(41), 7-14.
8. Volkov, V.A. (2018). Energy-saving traction frequen-cy-regulated synchronous-reactive engine. *Electromechanical and energy saving systems*, *3*(43), 8-23.
9. Volkov, A.V., & Kolesnikov, A.A. (2013). Energy-saving speed control of variable frequency asynchronous engine in acceleration and deceleration regimes. *Electronechnika*, *5*, 2-9.
10. Grunditz, E.A. (2016). *Design and Assessment of Battery Electric Vehicle Powertrain, with Respect to Performance, Energy Consumption and Electric Motor Thermal Capability*. Göteborg, Sweden: Chalmers University of Technology.

Енергозберігаюче керування тяговим частотно-регульованим асинхронним двигуном електромобіля

В. О. Волков

Національний технічний університет „Дніпровська політехніка“, м. Дніпро, Україна, e-mail: green_stone@ukr.net

Мета. Розробка енергозберігаючого керування тяговим частотно-регульованим асинхронним двигуном електромобіля, дослідження його електромеханічних і енергетичних процесів.

Методика. Методи варіаційного числення, Рунге-Кутта, математичного аналізу та інтерполяції, комп'ютерного моделювання.

Результати. Отримані аналітичні залежності для розрахунку загальних втрат потужності та енергії тягового частотно-регульованого асинхронного двигуна (ЧРАД) при режимах розгону й гальмування. За допомогою даних залежностей виконана кількісна оцінка зазначених втрат потужності та енергії, досліджені електромеханічні та енергетичні процеси цього ЧРАД для запропонованих енергозберігаючих і відомих (лінійного й параболічного виду) траєкторій швидкості.

Наукова новизна. Запропоновані енергозберігаючі тахограми для тягового ЧРАД при двох зонах регулювання (із постійним і ослабленим магнітним потоком), що дозволяють мінімізувати в пуско-гальмівних режимах його загальні втрати енергії. Отримані залежності, що дозволяють визначити енергозберігаючі значення швидкості електромобіля у сталих режимах.

Практична значимість. Застосування отриманих результатів забезпечує зниження непродуктивних втрат енергії тягового ЧРАД електромобіля та збільшення пробігу останнього на одній зарядці акумуляторної батареї.

Ключові слова: *тяговий асинхронний двигун, частотне регулювання, енергозберігаюче керування, електромобіль*

Энергосберегающее управление тяговым частотно-регулируемым асинхронным двигателем электромобиля

В. А. Волков

Национальный технический университет „Днепровская политехника“, г. Днепр, Украина, e-mail: green_stone@ukr.net

Цель. Разработка энергосберегающего управления тяговым частотно-регулируемым асинхронным двигателем электромобиля, исследование его электромеханических и энергетических процессов.

Методика. Методы вариационного исчисления, Рунге-Кутта, математического анализа и интерполяции, компьютерного моделирования.

Результаты. Получены аналитические зависимости для расчета общих потерь мощности и энергии тягового частотно-регулируемого асинхронного двигателя (ЧРАД) при режимах разгона и торможения. С помощью данных зависимостей выполнена количественная оценка указанных потерь мощности и энергии, исследованы электромеханические и энергетические процессы этого ЧРАД для предложенных энергосберегающих и известных (линейного и параболического вида) траекторий скорости.

Научная новизна. Предложены энергосберегающие тахограммы для тягового ЧРАД при двух зонах регулирования (с постоянным и ослабленным магнитным потоком), позволяющие минимизировать в пуско-тормозных режимах его общие потери энергии. Получены зависимости, позволяющие определить энергосберегающие значения скорости электромобиля в установившихся режимах.

Практическая значимость. Применение полученных результатов обеспечивает снижение непроизводительных потерь энергии тягового ЧРАД электромобиля и увеличение пробега последнего на одной зарядке аккумуляторной батареи.

Ключевые слова: *тяговый асинхронный двигатель, частотное регулирование, энергосберегающее управление, электромобиль*

Recommended for publication by S.M. Tykhovod, Doctor of Technical Sciences. The manuscript was submitted 28.08.18.